Preproglucagon (PPG) neurons in the hindbrain have IL-6 Receptor α (IL-6Rα) and show Ca^{2+} influx in response to IL-6.

Fredrik Anesten[1], Marie K Holt[2], Erik Schéle[1], Vilborg Pálsdóttir[1], Frank Reimann[3], Fiona M Gribble[3], Cecilia Safari[1], Karolina P Skibicka[1], Stefan Trapp[2], John-Olov Jansson[1]

Correspondence should be addressed to:
Prof. John-Olov Jansson
joj@neuro.gu.se
Medicinaregatan 11
Box 432
40530 Gothenburg, Sweden

[1] Department of Physiology, Institute of Neuroscience and Physiology, The Sahlgrenska Academy at the University of Gothenburg, S-413 45 Gothenburg, Sweden
[2] Centre for Cardiovascular and Metabolic Neuroscience, Department of Neuroscience, Physiology & Pharmacology, University College London, London, WC1E 6BT, UK
[3] Cambridge Institute for Medical Research, University of Cambridge, Addenbrooke's Hospital, Hills Road, Cambridge, CB2 0QQ, UK

Keywords: IL-6, IL-6Rα, PPG, GLP-1, hindbrain

Abstract

Neuronal circuits in the hypothalamus and hindbrain are of importance for control of food intake, energy expenditure and fat mass. We have recently shown that treatment with exendin-4 (Ex-4), an analogue of the pro-glucagon derived molecule glucagon-like peptide 1 (GLP-1), markedly increases mRNA-expression of the cytokine interleukin-6 (IL-6) in the hypothalamus and hindbrain, and that this increase partly mediates the suppression of food intake and body weight by Ex-4. Endogenous GLP-1 in the central nervous system (CNS) is produced by preproglucagon (PPG) neurons of the nucleus of the solitary tract (NTS) in the hindbrain. These neurons project to various parts of the brain, including the hypothalamus. Outside the brain, IL-6 stimulates GLP-1 secretion from the gut and pancreas.

In this study, we aim to investigate whether IL-6 can affect GLP-1 producing PPG neurons in the NTS in mouse hindbrain via the ligand binding part of the IL-6 receptor, IL-6 Receptor-α (IL-6Rα).

Using immunohistochemistry, we found that IL-6Rα was localized on PPG neurons of the NTS. Recordings of these neurons in GCaMP3/GLP-1 reporter mice showed that IL-6 enhances cytosolic Ca^{2+} concentration in neurons capable of expressing PPG. We also show that the Ca^{2+} increase originates from the extracellular space. Furthermore, we found that IL-6Rα was localized on cells in the caudal hindbrain expressing immunoreactive NeuN (a neuronal marker) or CNPase (an oligodendrocyte marker).

In summary, IL-6Rα is present on PPG neurons in the NTS, and IL-6 can stimulate these cells by increasing influx of Ca^{2+} to the cytosol from the extracellular space.

Introduction

It is well established that interleukin-6 (IL-6) contributes to stimulation of the innate immune system and induction of inflammation (1). In addition, IL-6 is important for the decreased appetite, enhanced energy metabolism and increased body temperature often observed during disease (6, 36). During inflammation and disease IL-6, along with other cytokines, acts via nervous afferents to induce a disease response in the brain (33). During more severe disease, circulating cytokines in the blood stream are thought to act on the circumventricular organs to induce a more pronounced disease response (9).

In healthy mice, IL-6 acts in lower concentrations than those observed during disease to cause a tonic decrease in body fat mass and an increase in energy expenditure (24, 38, 39). We, as well as others, have shown that IL-6^{-}/$^{-}$ mice develop mature onset obesity (24, 39). The anti-obesity effect of IL-6 in rodents is partly exerted at the level of the brain, presumably the hypothalamus and the hindbrain (22, 38, 39). Deficiency of IL-6 decreases leptin sensitivity, while overexpression of IL-6 in the brain enhances this parameter (12, 30, 39). Taken together, these findings suggest that IL-6 levels below those found in normal healthy individuals promote obesity (12, 24, 29, 39), while levels above normal may reduce appetite (7, 30). Therefore, it is important to identify which cells in the brain that express functional interleukin-6 receptor (IL-6Rα), and to determine whether these cells are localized in nuclei that regulate appetite and/or energy balance. Such a mapping of IL-6Rα has been done for body fat regulating centers in the hypothalamus (3, 31, 32, 40) while there are fewer studies on the hindbrain, another part of the brain regulating metabolic functions (14).

The proglucagon system includes proglucagon derived post-translational cleavage products such as Glucagon-like peptide 1 (GLP-1) (2). GLP-1 is an incretin with important effects on both blood glucose levels and fat mass. Outside the central nervous system (CNS), GLP-1 is mainly synthesized in the entero-endocrine L-cells in the distal gut and to some extent in the proximal gut (37). GLP-1 may also be produced by pancreatic α-cells (11). Within the CNS, GLP-1 is expressed in preproglucagon neurons in the nucleus of the solitary tract (NTS) in the brainstem. The anti-obesity effect of peripheral GLP-1 is assumed to be exerted via activation of vagal afferent fibres (10, 18). Whether these vagal afferents in turn activate the PPG neurons in the NTS to initiate central release of GLP-1 is currently under debate(17). Leptin and CCK are known to stimulate PPG neurons in the NTS, while several other appetite and/or peptides regulating body fat and food intake, including GLP-1 itself, have no effect (16, 17). These data are in line with the assumption that GLP-1 in NTS regulates body fat mass, and that this effect is exerted via interaction with other peptides regulating body fat and food intake such as leptin and CCK.

In recent studies we reported that treatment with Exendin-4 (Ex4), a long-lasting GLP-1 analogue, enhances the expression of IL-6 in both the hypothalamus and different parts of the hindbrain. We provided evidence that increased IL-6

110 expression mediates the anti-obesity effect of GLP-1 (28, 34). Similarly, it has
111 recently been shown that amylin, an anti-obesity and blood glucose regulating
112 hormone, induces central IL-6 production which in turn leads to increased leptin
113 sensitivity (21).
114
115 As discussed above, GLP-1 inhibits fat mass in part by stimulating IL-6 expression
116 (34). To further investigate possible interactions between GLP-1 and IL-6, we
117 sought to determine whether PPG neurons express functional IL-6Rα. Because
118 GLP-1 in the CNS is almost exclusively produced in the NTS, we stained for IL-6Rα
119 in brain slices from this area. Furthermore, we performed optical recordings
120 using Glu-Cre/Rosa26GCaMP3 transgenic mice to investigate whether IL-6 can
121 affect these neurons by modulation of Ca^{2+} influx and cytosolic Ca^{2+}
122 concentrations.
123
124 We have previously found that IL-6Rα is expressed in several different types of
125 neurons in hypothalamic nuclei (3, 31, 32). Besides neurons, the parenchymal
126 brain also consists of three different types of glial cells; astrocytes, microglia and
127 oligodendrocytes. In the present study we aimed to systematically elucidate
128 whether IL-6Rα in the NTS is expressed on neurons and/or different types of glial
129 cells.

130 Methods

131
132 *Animals*
133
134 Two transgenic C57BL6 mouse models were used in this study. Firstly, PPG
135 neurons were visualized using glucagon promoter (Glu)-YFP mice, in which
136 yellow fluorescent protein (YFP) is expressed under the control of the glucagon
137 promoter (23, 27). These mice were used for double staining of YFP and immuno-
138 reactive IL-6Rα. GCaMP3 mice were used for immuohistochemical validation of
139 the model. Standard wild type C57BL6 mice were used for the rest of the
140 immunohistochemistry. Glu-Cre/Rosa26-GCaMP3 transgenic mice expressing the
141 genetically encoded calcium indicator GCaMP3 in a Cre-dependent manner were
142 obtained by crossing Glu-Cre mice (26) with commercially available Rosa26-
143 GCaMP3 reporter mice (Jax strain 014538) (41) resulting in expression of the
144 genetically encoded Ca^{2+}-sensor GCAMP3 in PPG neurons (Fig. 1A).
145
146 Animals had free access to water and standard chow pellets (Tekland Global,
147 Harlan, The Netherlands), and were kept under standardized conditions on 12 h
148 light/dark cycle with *ad libitum* food. The local ethics committees for animal care
149 at the University of Gothenburg and University College London (UCL) approved all
150 animal procedures, respectively, and studies at UCL were conducted in accordance
151 with the U.K. Animals (Scientific Procedures) Act, 1986.
152
153 *Tissue preparation for immunohistochemistry*
154
155 Mice were deeply anaesthetized and perfused transcardially with heparinized
156 saline (50 IU/ml) followed by 4% paraformaldehyde in 0.1M phosphate buffer.
157 The brains were removed and post fixed in 4% paraformaldehyde in 0.1M

phosphate buffer containing 15% sucrose overnight at 4 °C. They were then transferred to a 30% sucrose solution in 0.1M phosphate buffer until sectioning. Coronal 20µm thick serial sections of the hypothalamus and hindbrain were cut using a Leica CM3050S cryostat (Leica Microsystem, Wetzlar, Germany) and stored in cryoprotectant solution (25% ethylene glycol; 25% glycerol; 0.05 m phosphate buffer). For GFP/GLP-1 co-staining, we instead used 30 um sections that were not post fixed in 4% paraformaldehyde in 0.1M phosphate buffer containing 15% sucrose overnight. Coronal sections corresponding to bregma -7,32 to -7,64 (interneural -3,52 to -3,84) were selected for staining.

Immunohistochemistry

Briefly, sections were rinsed in wash buffer (0.1M TrisHCl, pH 7.5, 0,15M NaCl, 0.2% Triton-X-100) and blocked for 1 h with TNB (Perkin Elmer, Waltham, MA, USA). Sections were incubated with primary antibodies (see supplementary table) for 2 days at 4 °C. After rinsing, sections were incubated for 1 h with secondary antibodies (see supplementary table) diluted in TNB blocking reagent. Sections were rinsed, and the IL-6Rα signal was developed by incubating the sections in Streptavidin-horseradish peroxidase in TNB blocking reagent (1:100, TSA™ System; Perkin Elmer) for 30 min and then with biotinyl-tyramide in amplification diluent (1:50, TSA™ System; Perkin Elmer). Following signal amplification, sections were stained with Streptavidin Alexa fluor 568-conjugate (1:250, S11226; Molecular Probes, Carlsbad, CA, USA). After a further wash, cell nuclei were stained with DAPI (1:5000, D1306; Molecular Probes) for 15 min, rinsed and mounted in mounting medium containing prolong gold antifade (P36930; Molecular Probes). As a control for the secondary antibodies, some sections were incubated with mismatching primary and secondary antibodies, resulting in negative staining (as a control for unwanted cross-reactivity). The rat anti-IL-6α antibody used in the present studied has been validated in several earlier studies (31, 32). Primary antibodies, their dilutions and catalogue numbers, as well as the manufacturers providing them are listed in Table 1.

Confocal microscopy and cell counting

Images of the stained sections were obtained using either a confocal microscope system (LSM 700; ZEISS, Oberkochen, Germany), together with a Plan APO ×63 A/1.40 oil lens (for close-up pictures) or a Plan Fluor ×20/0.75 lens (for anatomical overview pictures) and a solid-state laser. For co-localization between IL-6rα and GLP-1, focus stacking was used to achieve a greater depth of field and as such make it possible to more accurately detect possible co-localization. NTS YFP-labeled cells and IL6-rα-positive cells were quantified from at least 4 20 um sections per brain. Triple channel confocal images (to cover the entire NTS) were generated with a Plan Fluor ×20/0.75 lens and a solid-state laser. A tile scan of 3x3 tiles was obtained from the center of the NTS, covering the entirety of the nucleus. Neurons were considered IL-6Rα-labeled when the staining was clearly above background. The emission spectrum of the secondary fluorescent antibody is well known. By adjusting the splits of the confocal microscope, the signal of the

fluorophore was maximized while minimizing background fluorescence. The evaluation of IL-6Rα-labeling was done with the cell nucleus in the plane of focus.

Calcium imaging

Glu-Cre/Rosa26-GCaMP3 transgenic mice express the calcium indicator GCaMP3 in PPG neurons selectively. To confirm that GCaMP3 positive cells in the NTS produce GLP-1, double immunofluorescence was carried out with an anti-GFP antibody (Abcam) to detect GCaMP3 (25), and an anti-GLP-1 antibody (Bachem) to detect GLP-1 (15). As shown in Fig 1 B-D, the anti-GLP-1 antibody detected essentially all GCaMP3/GFP positive cells, but also cells that were not GCaMP3/GFP positive. This could indicate that visualization of GCaMP3/GFP expressing cells has incomplete penetrance, e.g due to lack of IL-Ra in about 60% of GLP-1 expressing cells (Fig 2G). Alternatively, the GLP-1 antibody may bind nonspecifically to additional cells that do not have GLP-1 and GCaMP3 expression and thereby are not stained. All cells expressing GCaMP3 were positive for GLP-1. On the day of recording mice underwent deep terminal anaesthesia using isofluorane. The brainstem was removed and placed in ice-cold high-magnesium/low-calcium artificial cerebrospinal fluid (ACSF) (composition in mM: 2.5 KCl, 200 sucrose, 28 $NaHCO_3$, 1.25 NaH_2PO_4, 7 Glucose, 7 $MgCl_2$, 0.5 $CaCl_2$; pH 7.4). 200µm thick coronal sections were cut on a vibratome (Campden Instruments) and left to incubate in high-magnesium/low-calcium recovery solution (in mM: 3 KCl, 118 NaCl, 25 $NaHCO_3$, 1.2 NaH_2PO_4, 2.5 Glucose, 7 $MgCl_2$, 0.5 $CaCl_2$; pH 7.4) at 34^{0}C for 45 minutes. Subsequently, the sections were transferred to standard ACSF (in mM: 3 KCl, 118 NaCl, 25 $NaHCO_3$, 10 Glucose, 1 $MgCl_2$, 2 $CaCl_2$; pH7.4) and left to incubate at 34^{0}C for a minimum of 30mins before imaging. All solutions were constantly bubbled with 95% O_2/5% CO_2. Imaging was performed on a Zeiss Axioskop widefield microscope using a 40x water immersion lens, CCD camera (Q-click; QImaging) and a LED light source (CoolLED pE300^{white}). Sections were continuously superfused with standard ACSF at 32^{0}C at a flow rate of 3-4ml/min. GCaMP3 was excited every 5 seconds for 250ms at 460nm+/-25nm. Regions of interest (ROIs) and an area representing background fluorescence were outlined and the mean pixel intensity calculated for each ROI. Background fluorescence was subtracted from each ROI and recordings are presented as $\Delta F/F_0$ with F_0 being the average intensity over 5 minutes prior to the stimulus and ΔF being the fluorescence intensity minus F_0. Quantifications were made by calculating the relative change in fluorescence between the fluorescent intensity in the absence of drug ($F_{no\text{-}drug}$) and the peak fluorescent intensity (F_{peak}): $(F_{peak}-F_{no\text{-}drug})/F_{no\text{-}drug}$. $F_{no\text{-}drug}$ was defined as the average of 1 minute before drug response onset and 1 minute after recovery from the response. IL-6 was dissolved in water and added directly to the ACSF. For recordings in the nominal absence of Ca^{2+}, Ca^{2+} was replaced with Mg^{2+}. All sections were exposed to 2nM IL-6, followed by a second exposure to IL-6 in 0mM Ca^{2+}, and finally exposed again to 2nM IL-6 in standard ACSF. Data are reported as mean±SEM. Statistics were analyzed using one-way ANOVA and post-hoc comparisons were made using the Bonferroni method.

Results

254
255 **IL-6Rα immunoreactivity is present in the NTS and is co-localized with GLP-**
256 **1.**
257
258 Immunofluorescence staining of hindbrain sections from Glu-YFP mice revealed
259 YFP-positive neurons activated by the Glu promoter (in green) co-localized with
260 IL-6Rα immunoreactivity (in red)(Fig 2A-D). Three examples of cells expressing
261 both IL-6 Rα and YFP, are shown in Fig 2B and Fig 2D (orange arrows).
262 Orthogonal images made from z-stacks focused on single cells clearly identified
263 two cells with both IL-6 Rα and GLP-1 as shown in in Fig 2B and 2D. Orthogonal
264 images made from z-stacks, focused on single cells with only IL-6Rα (white arrow)
265 or only GLP-1 (green arrow), are shown in in Fig 2E and 2F, respectively. Cell
266 counting showed that 38,5 % of the GLP-1 positive cells of the NTS also stained
267 positively for IL-6Rα. Conversely, 13% of the IL-6Rα positive cells of the NTS also
268 stained positively for GLP-1 (Fig 2G). Use of separate filters on the same area of
269 the NTS, as seen in Fig 2D, verified the co-localization results described above (not
270 shown).
271
272 **PPG neurons in the NTS respond to IL-6 with an increase in intracellular**
273 **Ca^{2+}**
274
275 *In vitro* calcium imaging was performed using adult Glu-Cre/Rosa26-GCaMP3
276 mice to characterize the functional response of PPG neurons to IL-6 (Fig. 3).
277 Bath-application of 2nM IL-6 led to an 8%±1.5% increase in intracellular Ca^{2+} in
278 PPG neurons (Fig 3B). To determine the source of the increase in intracellular Ca^{2+}
279 experiments we repeated the exposures to IL-6, but in the absence of extracellular
280 Ca^{2+}. Removal of extracellular calcium strongly reduced the intracellular Ca^{2+} (Fig
281 3C; top panel) an effect that was reversed upon reintroduction of extracellular
282 Ca^{2+}. The fact that the effect of IL-6 was reduced by about 90 % in the absence of
283 extracellular Ca^{2+} suggests that Ca^{2+} influx is necessary for the response to IL-6
284 (Fig. 3C; bottom panel).
285
286 **IL-6Rα immunoreactivity in the NTS is present on neurons and**
287 **oligodendrocytes, but not on astrocytes or microglia.**
288
289 In the hindbrain, immunofluorescent co-staining revealed that IL-6Rα
290 immunoreactivity (in green) in many cells was co-localized with a marker for
291 neuronal nuclei (NeuN, in red) (Fig 4A-B; orange arrows). There were numerous
292 NeuN positive cells without IL-6Rα (Fig 4B, red arrows show examples).
293 Additionally, IL-6Rα immunoreactivity (in green) co-localized in many cells with a
294 marker for oligodendrocytes (CNP:ase, in red). (Fig 4C-D; orange arrows show
295 examples). There were IL-6Rα positive cells without CNP:ase (white arrows show
296 examples). In contrast, IL-6Rα immunoreactivity was not co-expressed with
297 markers for microglia (Iba-1; Fig 5A-B) or astrocytes (GFAP; Fig 5C-D). The co-
298 localization between IL-6Rα and the four cellular markers was verified in a focus
299 stacking projection (Fig panels 4B, 4D, 5B, 5D).
300 Cell counting showed that 30 % of the cells expressing NeuN and CNP:ase were
301 also IL-6Ra positive. Conversely, 60% and 30% of the IL-6Rα positive cells, were

302 also positive for NeuN and CNP:ase, respectively. There was no co-localization
303 between GFAP and Iba-1 on one hand and IL-6Rα on the other (Table 2).
304
305 ## Discussion
306
307 It has previously been shown that IL-6 in CNS is of importance in regulation of
308 energy metabolism, and that IL-6 acts at the CNS level to decrease fat mass (20,
309 31, 34). IL-6^{-}/$^{-}$ mice develop mature onset obesity as well as insulin and leptin
310 resistance (24, 38). GLP-1 analogues, like Exendin-4 (Ex4), have also been shown
311 to decrease fat mass by acting at the CNS level (15). Ex4 is widely used as a
312 treatment for type 2 diabetes, where the beneficial side effects include mild weight
313 loss (10). Recently liraglutide, another GLP-1 analogue, has been used for
314 treatment of obesity *per se* (19). We have previously shown that
315 intracerebroventricular injections of Ex4 increases IL-6 mRNA levels both in
316 several parts of the hindbrain and in the hypothalamus, and that IL-6 is mediating
317 the anti-obesity effect exerted by this GLP-1 analogue (28, 34). These findings led
318 us to further study the possible interactions between these two neuromodulators,
319 to elucidate how they may interact to decrease fat mass.
320
321 Our present finding that IL-6Rα is expressed in PPG neurons in the NTS of the
322 hindbrain indicates that IL-6 has the capacity to influence GLP-1 expressing
323 neurons in the CNS via direct effects on IL-6Rα located on these neurons, in a
324 similar way as shown for leptin (16). As noted above, treatment with a GLP-1
325 analog increases the levels of IL-6 mRNA in the hypothalamus and the hindbrain
326 (34). Taken together, these findings are in line with a bidirectional interaction
327 between PPG neurons and IL-6 neurons. Such interactions are common in
328 biological context, and there are both general (4) and specific (13) examples of
329 this. However, further studies are needed to investigate if there is a bidirectional
330 interaction between GLP-1 and IL-6 producing cells, and if so, the nature of this
331 interaction.

332 Whilst results obtained by immunohistochemistry should always be interpreted
333 with caution, there is good reason to believe the co-localization between GLP-1
334 and IL-6Rα observed herein is valid. Firstly, we have previously identified IL-6Rα
335 by use of two independent antibodies (31, 32). Secondly, the Glu-YFP transgenic
336 mouse used here has been thoroughly validated (16, 23, 27, 28). Thirdly, the co-
337 staining was verified using focal stacking as well as three-dimensional analysis
338 seen in Fig 2B and D-F. Finally, the fact that PPG/GLP-1 expressing cells (identified
339 by both glucagon promoter activity and GLP-1 immunoreactivity) in the NTS
340 responded to addition of IL-6 strongly support that these cells express functional
341 IL-6Rα. Taken together, these methods make it reasonable to believe that the co-
342 staining shown is reliable.

343 GCaMP3 recordings revealed that adding IL-6 to mouse acute hindbrain sections
344 resulted in an influx of Ca^{2+} in PPG neurons, similarly to what has previously been
345 shown in hippocampal neurons (25). Our finding that IL-6 seems to stimulate
346 PPG neurons adds further information concerning the interaction between these
347 substances. We have previously shown that i.c.v injections of Ex4 in rat causes an
348 increase in IL-6 mRNA (34) and we show here that IL-6 in turn can stimulate PPG

349 neurons. One possible interpretation is that a GLP-1 analogue like Ex4 can
350 stimulate endogenous GLP-1 secretion, acting on NTS PPG neurons via IL-6. It has
351 been shown that GLP-1 itself cannot activate these PPG neurons (16). This would
352 constitute a feed forward effect, a type of effect seen for instance in connection to
353 immune stimulation. Further studies are needed to investigate this issue.

354 It should be noted that IL-6 outside the brain has been found by Donath and
355 coworkers to stimulate the secretion of GLP-1 from L-cells of the gut and α-cells of
356 the pancreas (11). Our current data suggest that IL-6 also stimulates a third GLP-1
357 expressing cell type, the PPG neurons in the NTS. It is currently unclear whether
358 circulating IL-6 or IL-6 produced locally in the brain influences PPG neurons in the
359 NTS. Circulating IL-6 may not cross the blood brain barrier, and therefore not
360 reach the NTS. Unlike e.g the area postrema, the NTS is not a circumventricular
361 organ and thus cannot be affected directly by peripherally produced peptides like
362 IL-6 (5). The fact that IL-6 levels in the cerebrospinal fluid often are higher than in
363 the blood circulation, also argues that IL-6 found in the brain is produced locally
364 rather than in the periphery (35).
365
366 We have previously reported that IL-6Rα is expressed in important energy-
367 regulatory neurons in the paraventricular nucleus (PVN) (3), in the arcuate
368 nucleus (ARC) (31) and in the lateral hypothalamic area (LHA) of the
369 hypothalamus (32). Neurons expressing IL-6Rα have been reported to express
370 several neuropeptides with energy balance regulating potential, such as TRH, CRH,
371 oxytocin, MCH, orexin, NPY and a-MSH (3, 31, 32). Here we show that IL-6Rα is
372 expressed in parts of the brainstem as well as in the hypothalamus.
373
374 There was no obvious co-localization between IL-6Rα and markers for astrocytes
375 and microglia, although it cannot be completely ruled out that IL-6Rα and the
376 markers are localized in different compartments within the same cell. In contrast,
377 we found CNPase immunoreactivity in about 30 % of the IL-6Rα positive cells of
378 the NTS. Therefore, IL-6Rα seems to be present on oligodendrocytes in this
379 nucleus. This is in accordance with previous findings that IL-Rα can be found on
380 oligodendrocytes in humans with multiple sclerosis as well as healthy controls (8).
381 Moreover, we found that a large part (about 60%) of the cells that expressed IL-
382 6Rα in the NTS also expressed the neuronal marker NeuN. These findings from
383 the caudal hindbrain are in line with results obtained from different parts of the
384 hypothalamus (3, 31, 32). Taken together, these results indicate that IL-6 exerts its
385 effects in caudal parts of the hindbrain and in the hypothalamus of healthy mice
386 primarily on neurons and oligodendrocytes.
387
388 In conclusion, our present findings show stimulation by IL-6 of PPG neurons and
389 localization of IL-6Rα on these cells. In the caudal hindbrain of healthy mice, IL-
390 6Rα is expressed on neurons and oligodendrocytes, while we found no evidence of
391 expression on astrocytes and microglia.
392
393
394 ## Perspectives and Significance
395

In a previous study we found evidence that GLP-1 stimulates IL-6 expression in the CNS, and that IL-6 may mediate the anti-obesity effects of GLP-1 The present findings demonstrate that IL-6 in turn activates PPG neurons in the NTS. Given that GLP-1 stimulates IL-6 expression, there is a possibility for bidirectional interaction between cells producing GLP-1 and IL-6 In the CNS. Alternatively, IL-6 produced in the periphery, may affect GLP-1 producing neurons in the CNS, as it has been shown to activate L-cells in the gut and alpha cells in the pancreas. The present findings are of clinical interest given that both GLP-1 analogues and IL-6 receptor blockers are used for treatment in humans.

Acknowledgements

We thank the Centre for Cellular Imaging at the University of Gothenburg for the use of imaging equipment, as well as support received from Julia Fernandez-Rodriguez, Maria Smedh and Carolina Tängemo. We also thank Edwin Gidestrand for assistance with immunohistochemistry.

This work was supported by grants from Swedish Research Council (K2016–54X-09894–19-3, 2011-3054 and 325–2008-7534), Johan och Jakob Söderbergs Foundation, Marcus Borgströms Foundation, Nilsson-Ehle Foundation, NovoNordisk Foundation, Novo Nordisk Foundation Excellence project grant (to KPS), Inga-Britt och Arne Lundbergs Foundation, Swedish Medical Society, Swedish Society for Medical Research, Kungl och Hvitfeldtska Foundation, EC FP7 funding (Health-F2–2010–259772, FP7/2007–2013 Grant Agreement 245009, Full4Health FP7-KBBE-2010–4- 266408, TORNADO [grant 222720]). MK Holt holds a UCL Graduate Research Fellowship and S Trapp is supported by a grant from the MRC UK (MR/J013293/2)

References

1. **Arora S, and Anubhuti**. Role of neuropeptides in appetite regulation and obesity--a review. *Neuropeptides* 40: 375-401, 2006.
2. **Baggio LL, and Drucker, DJ**. Biology of incretins: GLP-1 and GIP. *Gastroenterology* 132: 2131-2125, 2007.
3. **Benrick A, Schéle, E, Pinnock, SB, Wernstedt-Asterholm, I, Dickson, SL, Karlsson-Lindahl, L, and Jansson, JO**. Interleukin-6 gene knockout influences energy balance regulating peptides in the hypothalamic paraventricular and supraoptic nuclei. *Journal of Neuroendocrinology* 21: 620-628, 2009.
4. **Blalock JE**. A Molecular Basis for Bidirectional Communication Between the Immune and Neuroendocrine Systems. *Physiological Reviews* 69: 1989.
5. **Borison HL**. Area postrema: Chemoreceptor circumventricular organ of the medulla oblongata. *Progress in Neurobiology* 32: 351-390, 1989.
6. **Cahlin C, Körner, A, Axelsson, H, Wang, W, Lundholm, K, and Svanberg, E**. Experimental cancer cachexia: the role of host-derived cytokines interleukin (IL)-6, IL-12, interferon-gamma, and tumor necrosis factor alpha evaluated in

442 gene knockout, tumor-bearing mice on C57 Bl background and eicosanoid-
443 dependent cachexia. *Cancer Research* 60: 5488-5493, 2000.
444 7. **Campbell IL, Erta, M, Lim, SL, Frausto, R, May, U, Rose-John, S, Scheller,**
445 **J, and Hidalgo, J**. Trans-signaling is a dominant mechanism for the pathogenic
446 actions of interleukin-6 in the brain. *J Neurosci* 34: 2503-2513, 2014.
447 8. **Cannella B, and Raine, CS**. Multiple sclerosis: Cytokine receptors on
448 oligodendrocytes predict innate regulation. *Annals of Neurology* 55: 46–57, 2004.
449 9. **Cartmell T, Poole, S, Turnbull, AV, Rothwell, NJ, and Luheshi, GN**.
450 Circulating interleukin-6 mediates the febrile response to localised inflammation
451 in rats. *The Journal of Physiology* 526: 653-661, 2000.
452 10. **Drucker DJ**. The role of gut hormones in glucose homeostasis. *J Clin Invest*
453 117: 24–32, 2007.
454 11. **Ellingsgaard H, Hauselmann, I, Schuler, B, Habib, AM, Baggio, LL,**
455 **Meier, DT, Eppler, E, Bouzakri, K, Wueest, S, Muller, YD, Hansen, AM,**
456 **Reinecke, M, Konrad, D, Gassmann, M, Reimann, F, Halban, PA, Gromada, J,**
457 **Drucker, DJ, Gribble, FM, Ehses, JA, and Donath, MY**. Interleukin-6 enhances
458 insulin secretion by increasing glucagon-like peptide-1 secretion from L cells and
459 alpha cells. *Nature Medicine* 17: 1481-1489, 2011.
460 12. **Flores MB, Fernandes, MF, Ropelle, ER, Faria, MC, Ueno, M, Velloso, LA,**
461 **Saad, MJ, and Carvalheira, JB**. Exercise improves insulin and leptin sensitivity in
462 hypothalamus of Wistar rats. *Diabetes* 55: 2554-2561, 2006.
463 13. **Friedman JM, and Halaas, JL**. Leptin and the regulation of body weight in
464 mammals. *Nature Medicine* 395: 763–770, 1998.
465 14. **Grill HJ, and Hayes, MR**. Hindbrain neurons as an essential hub in the
466 neuroanatomically distributed control of energy balance. *Cell Metabolism* 16: 296-
467 309, 2012.
468 15. **Hayes MR, Leichner, TM, Zhao, S, Lee, GS, Chowansky, A, Zimmer, D,**
469 **De Jonghe, BC, Kanoski, SE, Grill, HJ, and Bence, KK**. Intracellular signals
470 mediating the food intake-suppressive effects of hindbrain glucagon-like peptide-1
471 receptor activation. *Cell Metab* 2: 320-330, 2011.
472 16. **Hisadome K, Reimann, F , Gribble, FM, and Trapp, S**. Leptin directly
473 depolarizes preproglucagon neurons in the nucleus tractus solitarius: electrical
474 properties of glucagon-like Peptide 1 neurons. *Diabetes* 59: 1890-1898, 2010.
475 17. **Hisadome K, Reimann, F, Gribble, FM, and Trapp, S**. CCK Stimulation of
476 GLP-1 Neurons Involves α1-Adrenoceptor–Mediated Increase in Glutamatergic
477 Synaptic Inputs *Diabetes* 60: 2701-2709, 2011.
478 18. **Holst JJ**. The Physiology of Glucagon-like Peptide 1. *Physiol Rev* 87: 1409 –
479 1439, 2007.
480 19. **Iepsen EW, Torekov, SS, and Holst, JJ**. Therapies for inter-relating
481 diabetes and obesity - GLP-1 and obesity. *Expert Opin Pharmacother* 15: 2487-
482 2500, 2014.
483 20. **Jansson JO, Wallenius, K, Wernstedt, I, Ohlsson, C, Dickson, SL, and**
484 **Wallenius, V**. On the site and mechanism of action of the anti-obesity effects of
485 interleukin-6. *Growth Horm IGF Res* 13: S28-32, 2003.
486 21. **LeFoll C, Johnson, MD, Dunn-Meynell, AA, Boyle, CN, Lutz, TA, and**
487 **Levin, BE**. Amylin-induced central IL-6 production enhances ventromedial
488 hypothalamic leptin signaling. *Diabetes* 64: 1621-1631, 2015.
489 22. **Li G, Klein, RL, Matheny, M, King, MA, Meyer, EM, and Scarpace, PJ**.
490 Induction of uncoupling protein 1 by central interleukin-6 gene delivery is

491 dependent on sympathetic innervation of brown adipose tissue and underlies one
492 mechanism of body weight reduction in rats. *Neuroscience* 115: 879-889, 2002.
493 23. **Llewellyn-Smith IJ, Reimann, F, Gribble, FM, and Trapp, S**.
494 Preproglucagon neurons project widely to autonomic control areas in the mouse
495 brain. *Neuroscience* 28: 111-121, 2011.
496 24. **Matthews VB, Allen, TL, Risis, S, Chan, MH, Henstridge, DC, Watson, N,**
497 **Zaffino, LA, Babb, JR, Boon, J, Meikle, PJ, Jowett, JB, Watt, MJ, Jansson, JO,**
498 **Bruce, CR, and Febbraio, MA**. Interleukin-6-deficient mice develop hepatic
499 inflammation and systemic insulin resistance. *Diabetologia* 53: 2431-2441, 2010.
500 25. **Orellana DI, Quintanilla, RA, Gonzalez-Billault, C, and Maccioni, RB**.
501 Role of the JAKs/STATs pathway in the intracellular calcium changes induced by
502 interleukin-6 in hippocampal neurons. *Neurotox Res* 8: 295-304, 2005.
503 26. **Parker HE, Adriaenssens, A, Rogers, G, Richards, P, Koepsell, H,**
504 **Reimann, F, and Gribble, FM**. Predominant role of active versus facilitative
505 glucose transport for glucagon-like peptide-1 secretion. . *Diabetologia* 55: 2445–
506 2455, 2012.
507 27. **Reimann F, Habib, AM, Tolhurst, G, Parker, HE, Rogers, GJ, and Gribble,**
508 **FM**. Glucose sensing in L cells: a primary cell study. *Cell Metabolism* 8: 532-539,
509 2008.
510 28. **Richard JE, Farkas, I , Anesten, F, Anderberg, RH, Dickson, SL, Gribble,**
511 **FM, Reimann, F, Jansson, JO, Liposits, Z, and Skibicka, KP**. GLP-1 receptor
512 stimulation of the lateral parabrachial nucleus reduces food intake:
513 neuroanatomical, electrophysiological, and behavioral evidence. *Endocrinology*
514 155: 4356-4367, 2014.
515 29. **Ruderman NB, Keller, C, Richard, AM, Saha, AK, Luo, Z, Xiang, X, Giralt,**
516 **M, Ritov, VB, Menshikova, EV, Kelley, DE, Hidalgo, J, Klarlund Pedersen, B, and**
517 **Kelly, M**. Interleukin-6 regulation of AMP-activated protein kinase. Potential role
518 in the systemic response to exercise and prevention of the metabolic syndrome.
519 *Diabetes* 55: S48-52, 2006.
520 30. **Sadagurski M, Norquay, L, Farhang, J, D'Aquino, K, Copps, K, and**
521 **White, MF**. Human IL6 enhances leptin action in mice. *Diabetologia* 53: 525–535,
522 2010.
523 31. **Schéle E, Benrick, A, Grahnemo, L, Egecioglu, E, Anesten, F, Pálsdóttir,**
524 **V, and Jansson, JO**. Inter-relation between interleukin (IL)-1, IL-6 and body fat
525 regulating circuits of the hypothalamic arcuate nucleus. *Journal of*
526 *Neuroendocrinology* 25: 580-589, 2013.
527 32. **Schéle E, Fekete, C, Egri, P, Füzesi, T, Palkovits, M, Keller, É, Liposits, Z,**
528 **Gereben, B, Karlsson-Lindahl, L, Shao, R, and Jansson, JO**. Interleukin-6
529 receptor α is co-localised with melanin-concentrating hormone in human and
530 mouse hypothalamus. *J Neuroendocrinol* 24: 930-943, 2012.
531 33. **Schettini G, Grimaldi, M, Landolfi, E, Meucci, O, Ventra, C, Florio, T,**
532 **Scorziello, A, and Marino, A**. Role of interleukin-6 in the neuroendocrine system.
533 *Acta Neurol (Napoli)* 13: 361-367, 1991.
534 34. **Shirazi R, Palsdottir, V, Collander, J, Anesten, F, Vogel, H, Langlet, F,**
535 **Jaschke, A, Schürmann, A, Prévot, V, Shao, R, Jansson, JO, and Skibicka, KP**.
536 Glucagon-like peptide 1 receptor induced suppression of food intake and body
537 weight is mediated by central IL-1 and IL-6. *ProcNatlAcadSci* 110: 16199-16204,
538 2013.

35. **Stenlöf K, Wernstedt, I, Fjällman, T, Wallenius, V, Wallenius, K, and Jansson, JO**. Interleukin-6 Levels in the Central Nervous System Are Negatively Correlated with Fat Mass in Overweight/Obese Subjects. *JCEM* 88: 4379 – 4383, 2003.

36. **Strassmann G, Fong, M, Kenney, JS, and Jacob, CO**. Evidence for the involvement of interleukin 6 in experimental cancer cachexia. *J Clin Invest* 89: 1681-1684, 1992.

37. **Svendsen B, Pedersen, J, Albrechtsen, NJ, Hartmann, B, Toräng, S, Rehfeld, JF, Poulsen, SS, and Holst, JJ**. An analysis of cosecretion and coexpression of gut hormones from male rat proximal and distal small intestine. *Endocrinology* 156: 847-857, 2015.

38. **Wallenius K, Wallenius, V, Sunter, D, Dickson, SL, and Jansson, JO**. Intracerebroventricular interleukin-6 treatment decreases body fat in rats. *Biochem Biophys Res Commun* 293: 560-565, 2002.

39. **Wallenius V, Wallenius, K, Ahrén, B, Rudling, M, Carlsten, H, Dickson, SL, Ohlsson, C, and Jansson, JO**. Interleukin-6-deficient mice develop mature-onset obesity. *Nature Medicine* 8: 75-79, 2002.

40. **Vallières L, and Rivest, S**. Interleukin-6 is a needed proinflammatory cytokine in the prolonged neural activity and transcriptional activation of corticotropin-releasing factor during endotoxemia. *Endocrinology* 140: 3890-3903, 1999.

41. **Zariwala HA, Borghuis, BG, Hoogland, TM, Madisen, L, Tian, L, De Zeeuw, CI, Zeng, H, Looger, LL, Svoboda, K, and Chen, TW**. A Cre-dependent GCaMP3 reporter mouse for neuronal imaging in vivo. *J Neurosci* 32: 3131–3141, 2012.

Figure Legends

Table 1. Basic information about the primary and secondary antibodies used in this study.

Antibody	Dilution	Cat. No	Manufacturer

Rat anti-IL-6Rα	1:20	BAM18301	R&D Systems, Minneapolis, MN, USA
Rabbit anti-GFAP	1:200	Z 0334	DakoCytomation, Glostrup, Denmark
Rabbit anti-Iba1	1:200	019-19741	Wako Chemicals, Richmond, VA, USA
Mouse anti-CNP:ase	1:100	MAB326	Millipore, Billerica, MA, USA
Rabbit anti-NeuN	1:100	ABN78	Millipore, Billerica, MA, USA
Rabbit anti-GLP-1 (7-36) amide	1:200	T-4057	Peninsula Laboratories / Bachem, Torrance, CA, USA
Goat anti-rat biotin	1:1000	ab7096	abcam, Cambridge, UK
Donkey Alexa fluor 488-conjugated anti-rabbit IgG	1:250	A21206	Molecular Probes, Carlsbad, CA, USA
Rabbit Alexa fluor 488-conjugated anti-mouse IgG	1:250	A11059	Molecular Probes, Carlsbad, CA, USA
Donkey Alexa fluor 568-conjugated anti-rabbit IgG	1:250	A10042	Molecular Probes, Carlsbad, CA, USA
Donkey Alexa flour 568-conjugated anti-mouse IgG	1:250	A10037	Molecular Probes, Carlsbad, CA, USA

587
588
589
590
591
592
593
594
595
596
597
598
599
600 **Table 2.** Overlap between IL-6Rα positive cells and neuronal/glial cell markers.
601 Results of cell counting suggest that cells with markers for neurons (NeuN) and
602 oligodendrocytes (CNP:ase), but not astrocytes (GFAP) or microglia (Iba-1), are
603 responsive to IL-6 in the NTS of healthy mice.

	%		%
100x NeuN/IL-6Rα	58	**100x IL-6Rα/NeuN**	32
100x CNP:ase/IL-6Rα	28	**100x IL-6Rα/CNP:ase**	30
100x GFAP/IL-6Rα	0-2	**100x IL-6Rα/GFAP**	0-2
100x Iba-1/IL-6Rα	0-2	**100x IL-6Rα/Iba-1**	0-2

Figure 1: (A) PPG promoter (Glu)-Cre mice were mated with Rosa26 promoter-STOP-GCaMP3 mice. The Rosa26 promoter is active in most cell types. In cells with active PPG promoter, the CRE protein cleaved out the STOP sequence upstream of the GCaMP3 gene. This resulted in expression of the GCaMP3 protein and emission of green fluorescence after stimulation of Ca^{2+} influx into the cytosol, e.g after stimulation by IL-6. (B) Immunofluorescence showing anti-GLP-1 immunoreactivity in red in cells in the NTS of Glu-Cre-GCaMP3 mice. (C) Immunofluorescence showing anti-GFP immunoreactivity in green in cells in the NTS of Glu-Cre-GCaMP3 mice. (D) Cells in the NTS of mice with anti-GLP-1 immunoreactivity in red, anti-GFP immunoreactivity in green, demonstrating co-localization of the two markers (yellow).

Figure 2: Interleukin-6 receptor α (IL-6Rα) is co-localized with glucagon like peptide-1 (GLP-1) in the nucleus of the solitary tract (NTS) of the hindbrain. Immunohistochemistry showing IL-6Rα-immunoreactivity in red, GLP-1-immunoreactivity in green, and nuclear staining (DAPI) in blue in a coronal section of the mouse hindbrain. 2A and 2C show overviews of the NTS. 2B and 2D show magnifications of the areas indicated in 2A and 2C, respectively. One cell each in in 2B, D, E and F are subject to orthogonal analysis using z-stacks. Orange arrows indicate examples of co-localization between IL-6Rα and GLP-1. White and green arrows indicate examples of cells with only IL-6Rα (2E) and only GLP-1 (2F), respectively (2D). Results of cell counting concerning the interrelation between GLP-1 and IL-6Rα are shown in 2G. Roughly 38% of all GLP-1 positive cells also stain positively for IL-6Rα and roughly 16% of all IL-6Rα positive cells stain positively for GLP-1. Images were obtained using the confocal microscope system described in materials and methods. CC = central canal, NTS = nucleus of the solitary tract. Scale bars = 100 µm (overview), 10 µm (magnification).

Figure 3: Preproglucagon neurons in the NTS respond to IL-6 with a rise in intracellular Ca^{2+}
A) Representative image of GCaMP3 fluorescence in PPG neurons in the NTS. Scale bar = 20µm. B) Traces showing the increase in intracellular Ca^{2+} in response to 2nM IL-6. Grey = individual cells. Black = average trace. N=6. C) The rise in intracellular Ca^{2+} in response to IL-6 is dependent on influx of extracellular Ca^{2+}. Top panel: Representative trace showing the response to IL-6 (green bars) before, during, and after exposure to Ca^{2+}-free solution. Note that removal of extracellular

652 Ca^{2+} ($0Ca^{2+}$) also reduces the basal intracellular Ca^{2+} concentration. Bottom panel:
653 mean peak change in intracellular Ca^{2+} in the presence (grey bars, N=19 and 18,
654 respectively) and absence (white bar, N=28) of extracellular Ca^{2+}. *** indicates
655 $p<0.001$
656
657 **Figure 4: Interleukin-6 receptor α (IL-6Rα) is localized on neurons and**
658 **oligodendrocytes.**
659 Immunohistochemistry showing IL-6Rα-immunoreactivity in green, (NeuN
660 immunoreactivity in red (4A-B), CNPase immunoreactivity in red (4C-D) and
661 nuclear staining (DAPI) in blue in a coronal section of the mouse hindbrain. (4A,
662 C) Overview of the NTS, and (4B, D) magnification of the areas indicated in Fig 3A
663 and C. Examples of cells with both IL-6Rα and NeuN (4B, orange arrows), cells
664 with both IL-6Rα and CNPase (4D, orange arrows) as well as a cell only positive
665 for NeuN (Fig 4B, red arrows) or IL-6Rα (Fig 4D, white arrows) are shown.
666 Images were obtained using the confocal microscope system described in
667 materials and methods. CC = central canal. Scale bars = 100 µm (overview), 10 µm
668 (magnification).
669
670 **Figure 5: Interleukin-6 receptor α (IL-6Rα) is not localized on astrocytes or**
671 **microglia.**
672 Immunohistochemistry showing IL-6Rα-immunoreactivity in gren and nuclear
673 staining (DAPI) in blue (5A-D) in a coronal section of the hindbrain. Iba-1-
674 immunoreactivity (5A, B) and GFAP-immunoreactivity (5C, D) are shown in red.
675 (5A, C) overviews of the mouse NTS, and (5D) a magnification of the area
676 indicated in 5C. Figure 5B show examples of IL6-Rα-positive and negative
677 neurons. White arrows indicate cells containing IL6-Rα. There was no co-
678 localization between glial cell markers, GFAP and Iba-1 on one hand, and IL-6Rα
679 on the other. Images were obtained using the confocal microscope system
680 described in materials and methods. CC = central canal. Scale bars = 100 µm
681 (overview), 10 µm (magnification).

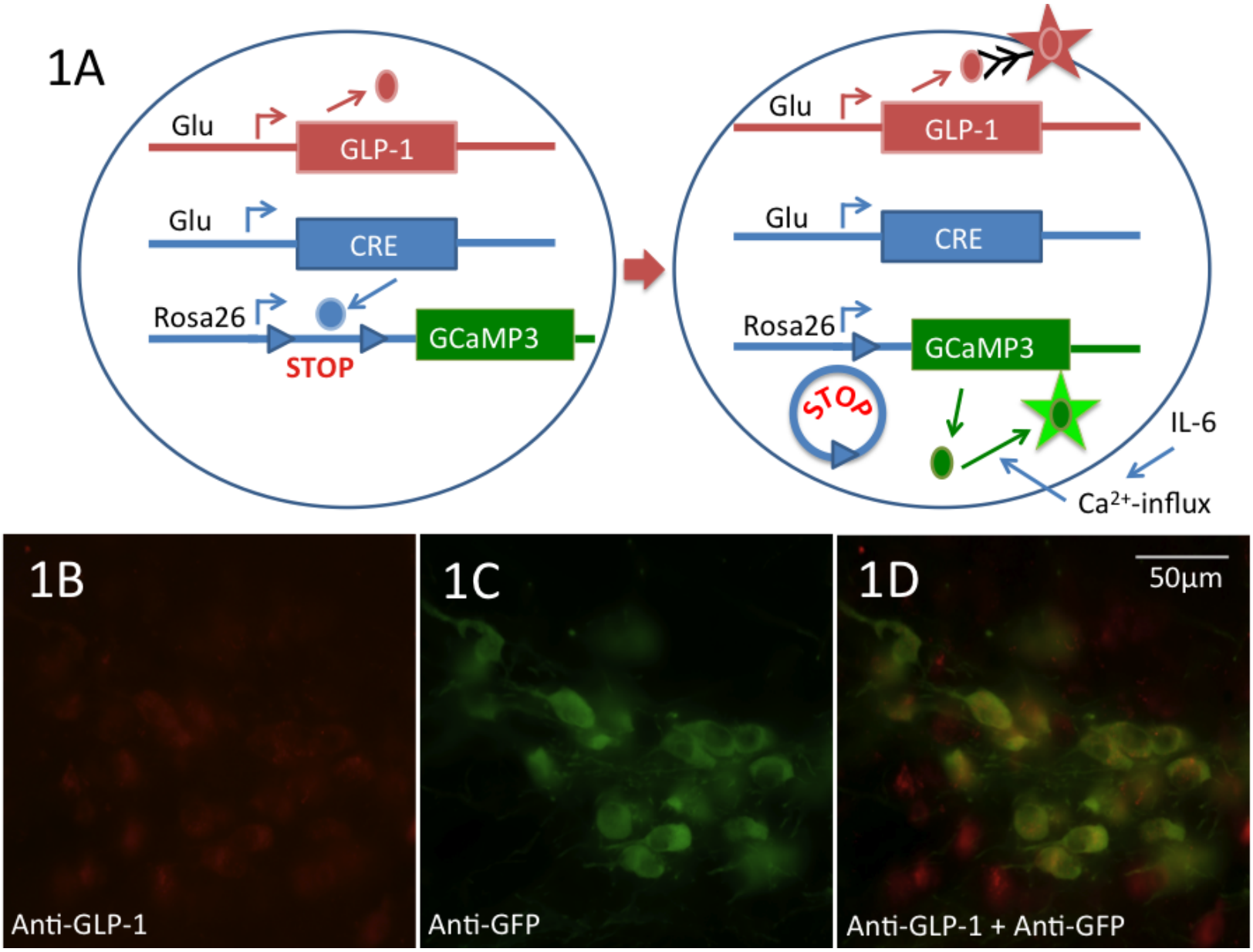
1A
Glu
GLP-1
Glu
CRE
Rosa26
GCaMP3
STOP
Glu
GLP-1
Glu
CRE
Rosa26
GCaMP3
STOP
IL-6
Ca2+-influx
1B
Anti-GLP-1
1C
Anti-GFP
1D
50µm
Anti-GLP-1 + Anti-GFP

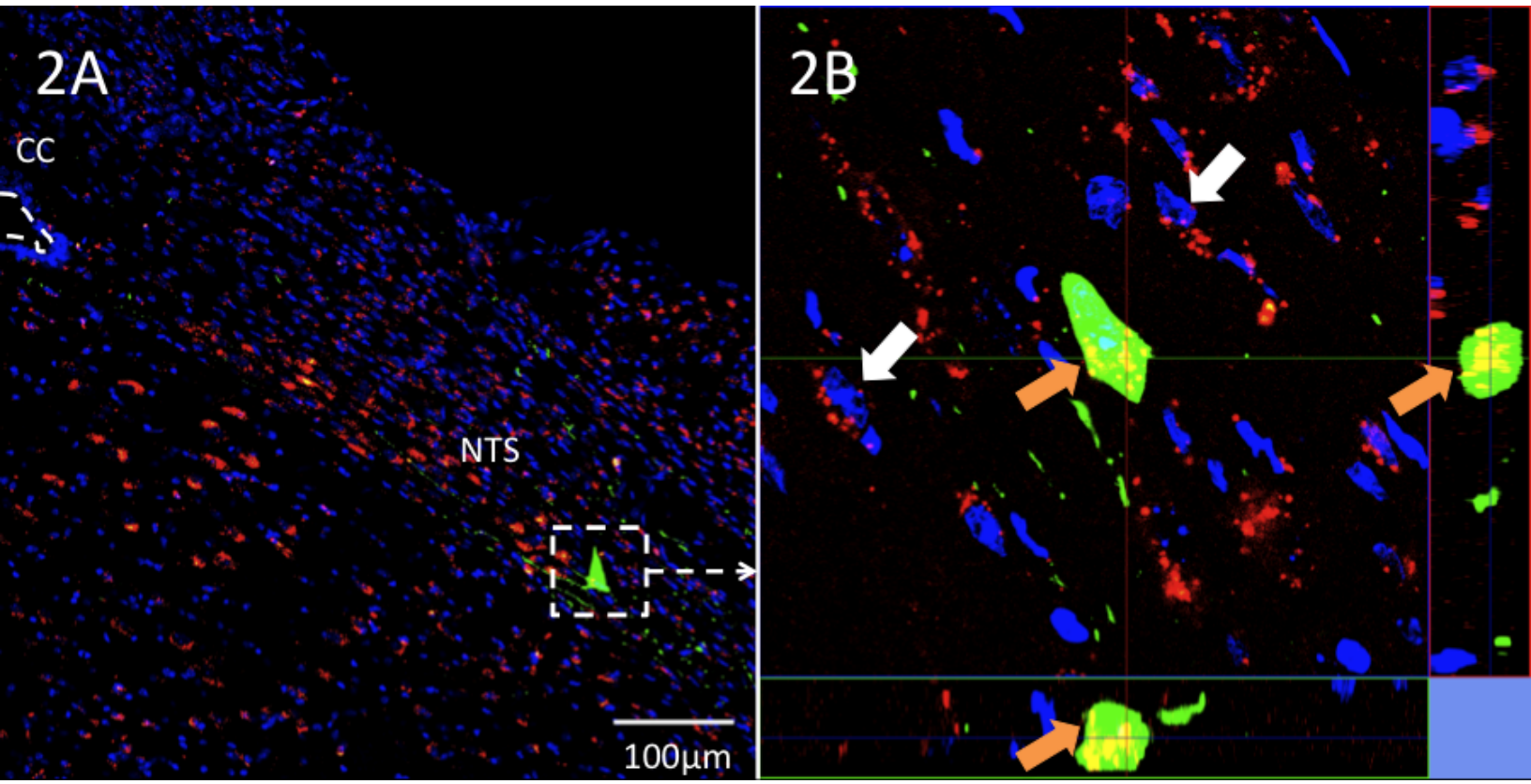
2A
CC
NTS
100µm
2B

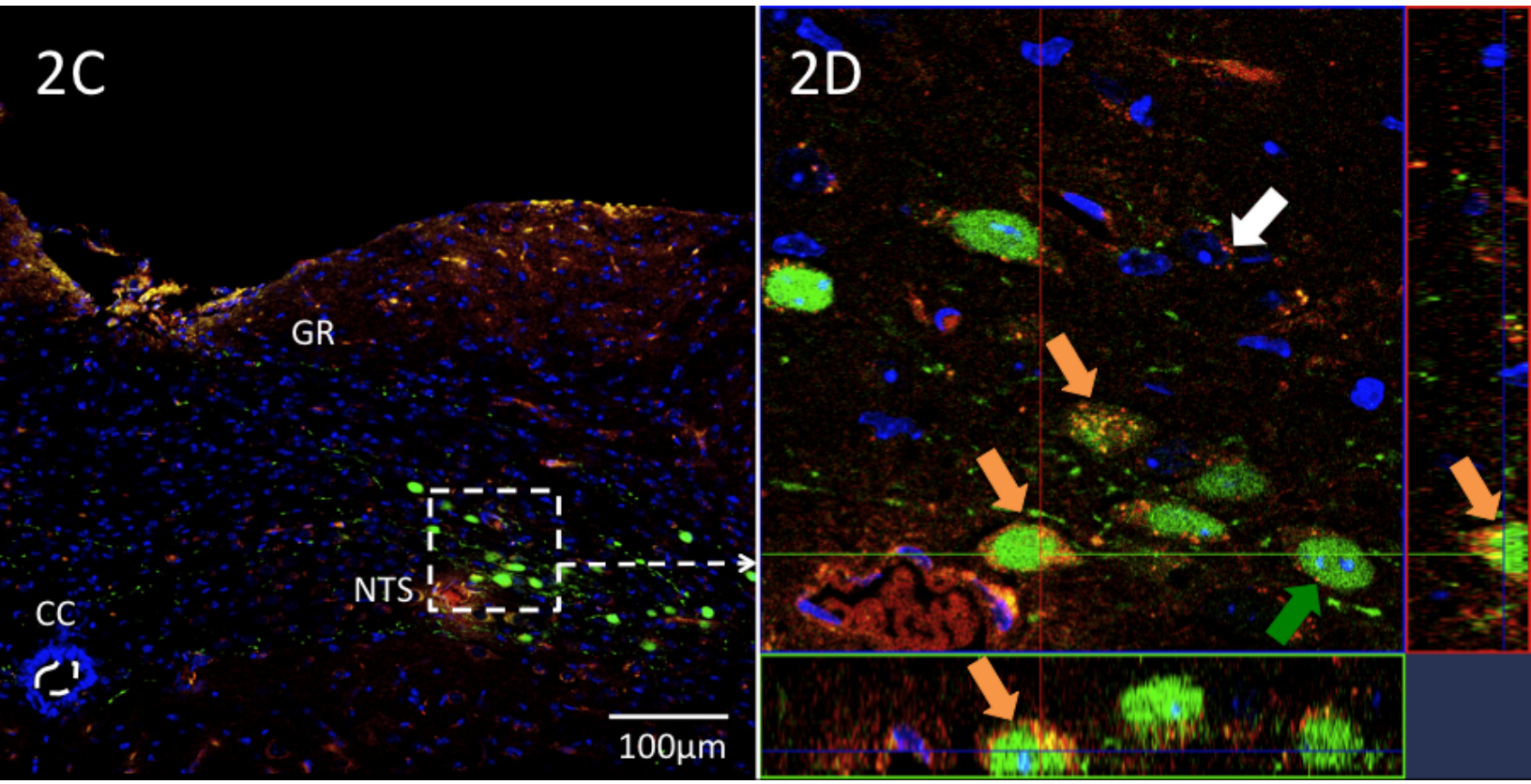
2C
GR
NTS
CC
100µm
2D

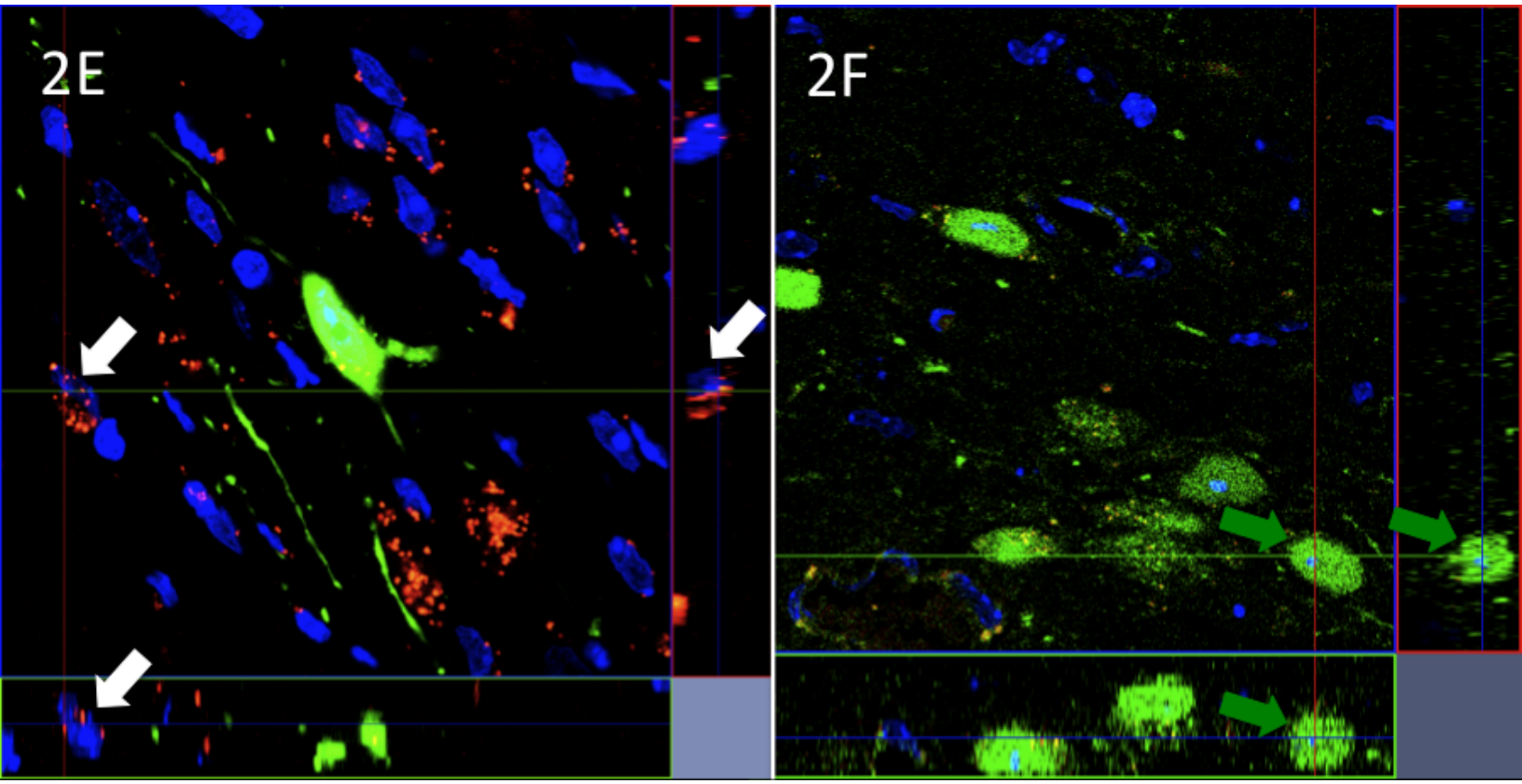
2E
2F

2G

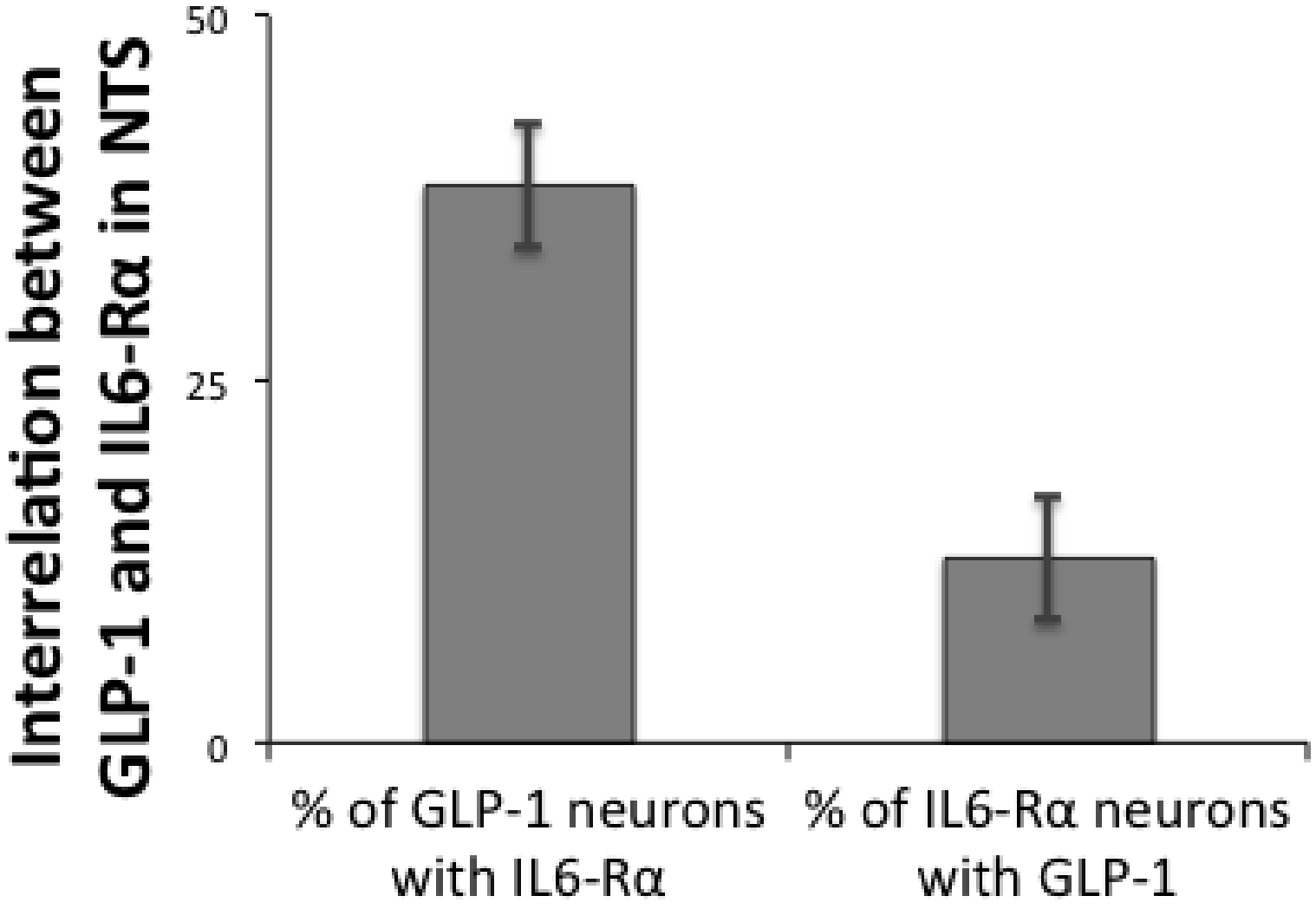
Interrelation between GLP-1 and IL6-Rα in NTS
50
25
0
% of GLP-1 neurons with IL6-Rα
% of IL6-Rα neurons with GLP-1

3

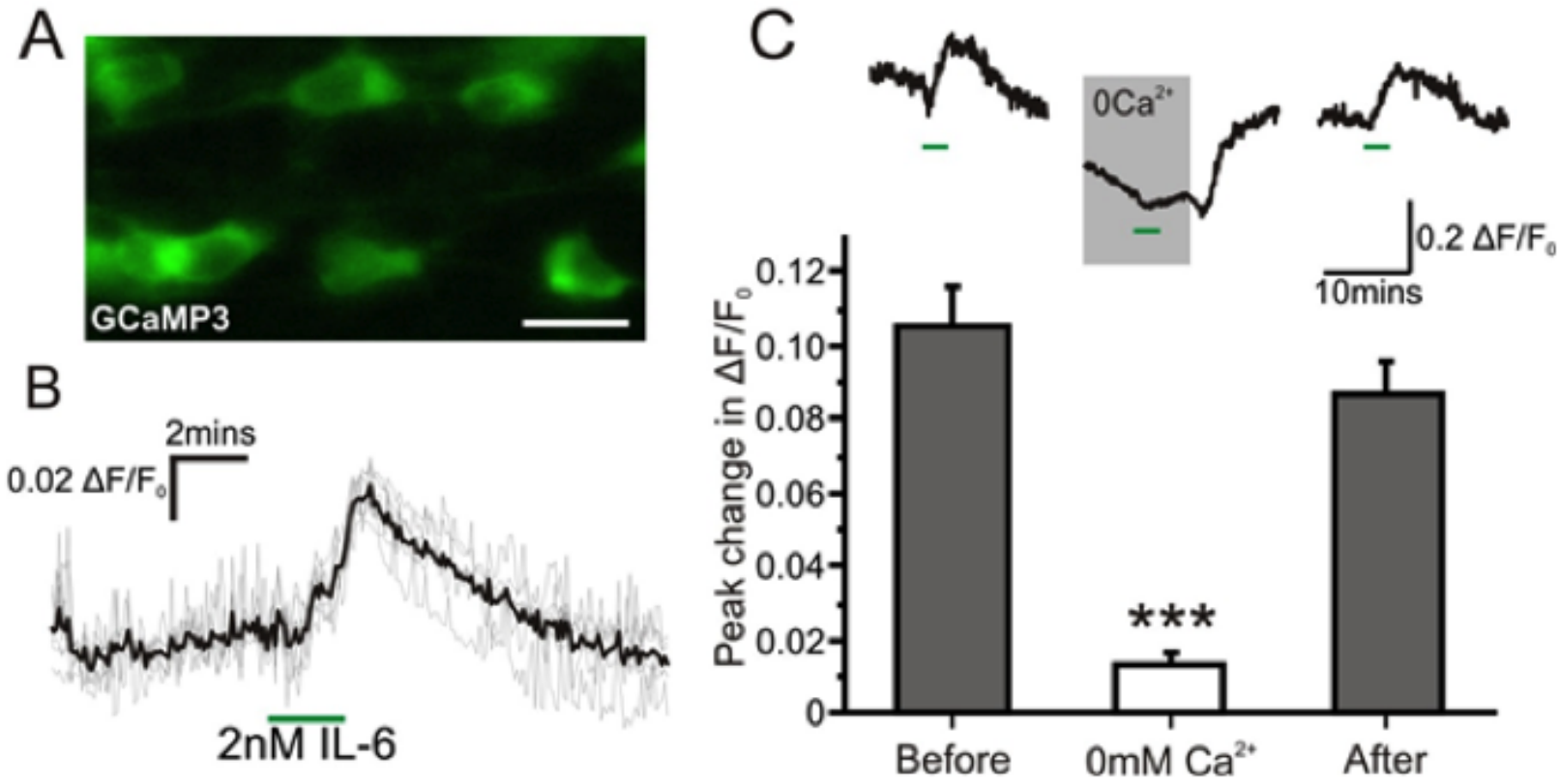
A
GCaMP3
B
2mins
0.02 ΔF/F0
2nM IL-6
C
0Ca2+
0.2 ΔF/F0
10mins
Peak change in ΔF/F0
0.12
0.10
0.08
0.06
0.04
0.02
0
***
Before
0mM Ca2+
After

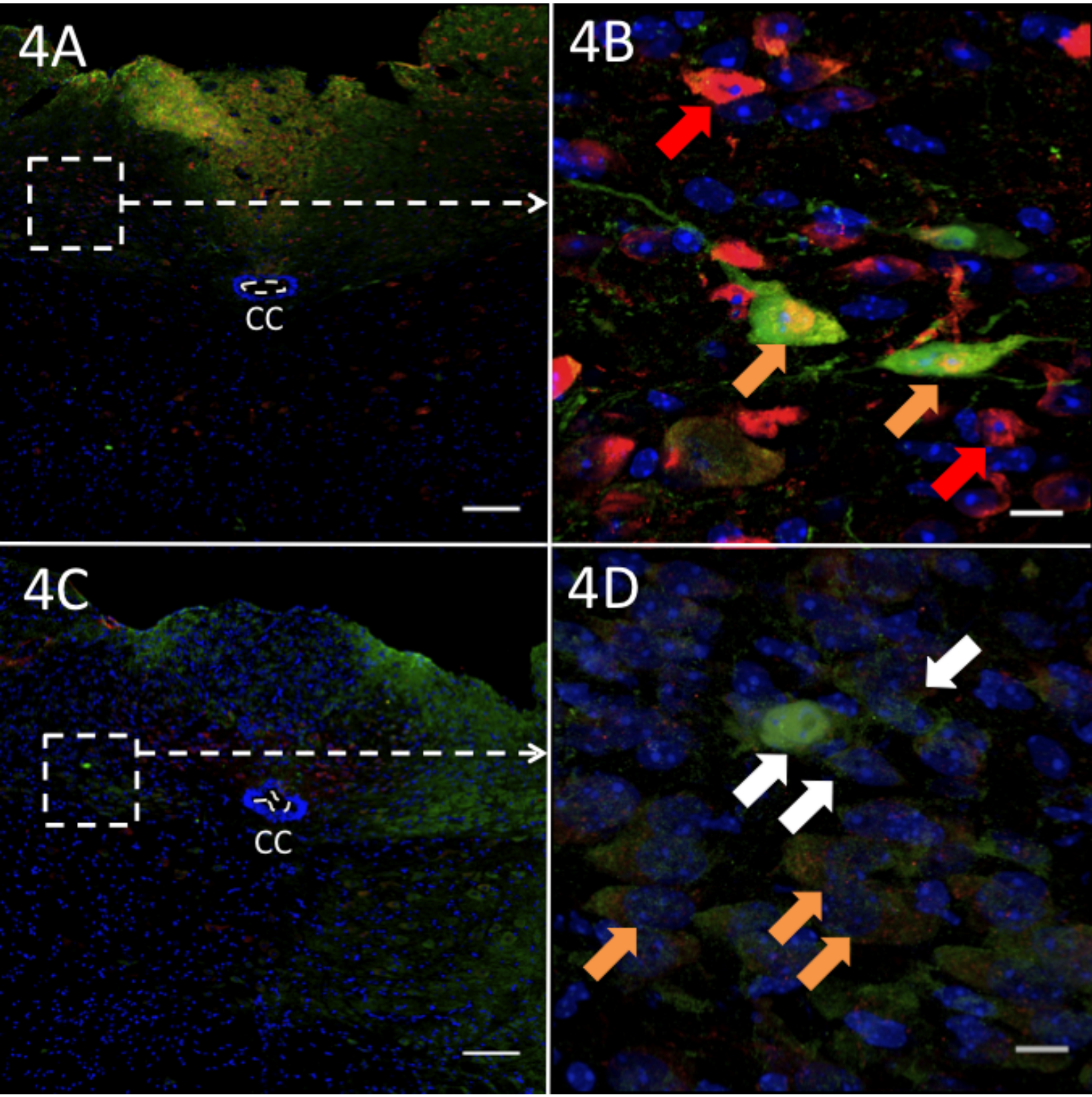
4A
CC
4B
4C
CC
4D

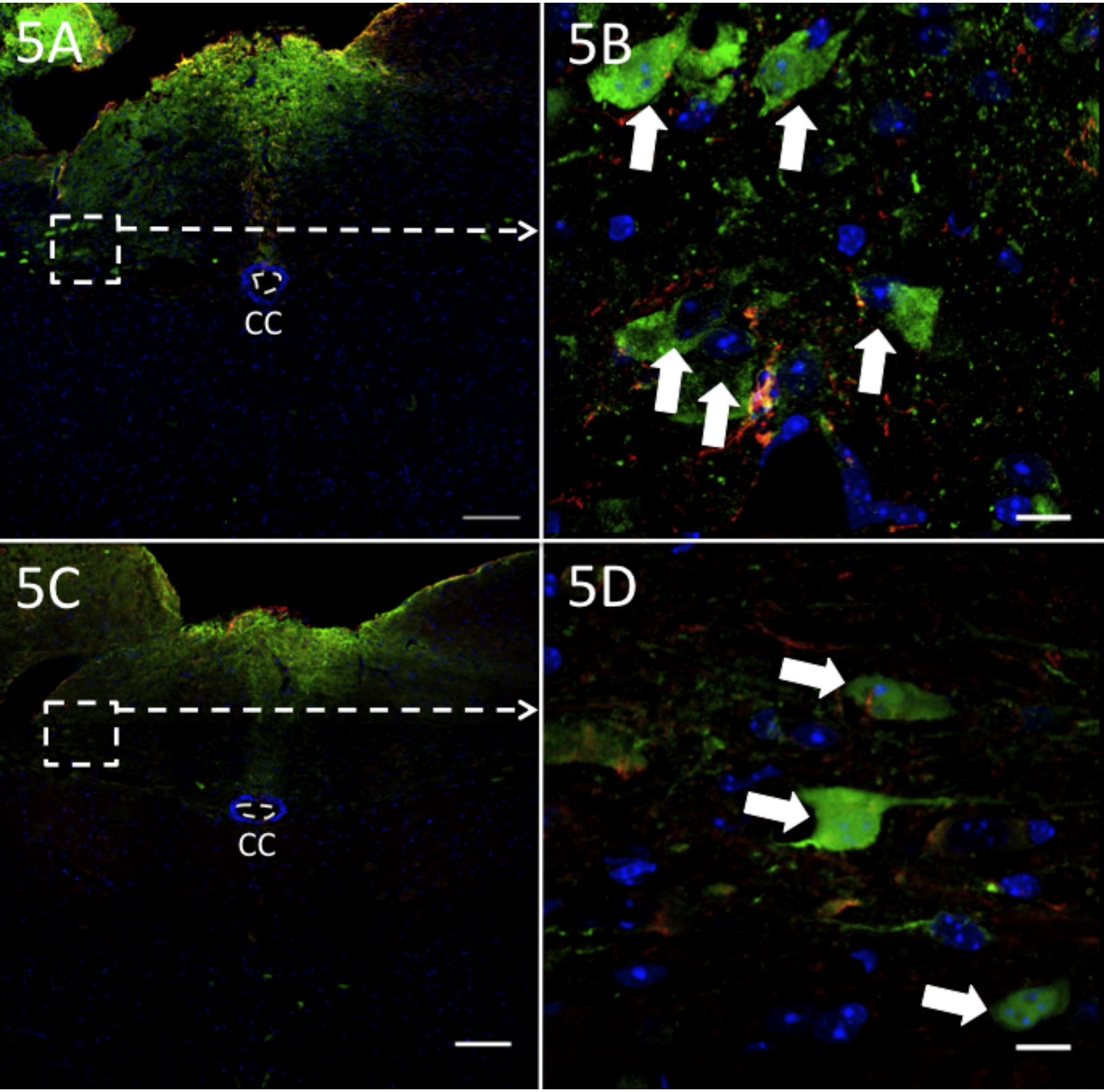
5A
CC
5B
5C
CC
5D